

AROMATICITY OF AZA AROMATIC MOLECULES: PREDICTION FROM HÜCKEL THEORY WITH MODIFIED PARAMETERS

Inge M. Sutjahja^{a,*}, Yuanita P. D. Sudarso^b, Shofi Dhiya ‘Ulhaq^a and Erik Bekti Yutomo^a

^aDepartment of Physics, Faculty of Mathematics and Natural Sciences, Institut Teknologi Bandung, 40132 Bandung, Indonesia

^bDepartment of Physics, Faculty of Information Technology and Science, Parahyangan Catholic University, 40141 Bandung, Indonesia

Recebido em 14/10/2022; aceito em 11/11/2022; publicado na web 27/01/2023

Hückel theory is a simple and powerful method for predicting the molecular orbital and the energy of conjugated molecules. However, the presence of nitrogen atoms in aza aromatic molecules alters the Coulomb and resonance integrals owing to the difference in electronegativity between nitrogen and carbon atoms. In this study, we focus on acridine and phenazine. Further correction is implemented based on the ring current model, thus revealing the change in resonance integral for the carbon-carbon bond along the bridge of the molecule. The Hamiltonian of the π -electron system in the Hückel method is solved using the HuLiS software. Various geometry-based aromaticity indices are used to obtain the aromaticity indices of the two non-equivalent rings. For further evaluation, the results for bond lengths are used to calculate the associated bond energy. Considering the carbon-hydrogen (CH) bonds, the total molecular energy is compared with the experimental heats of formation for a number of benzenoid hydrocarbons and aza aromatics, in addition to the two studied molecules. Finally, the correlation between the nitrogen atom on the aromaticity index and the ring energy content is evaluated to determine to which extent the Hückel model agrees with previous experimental and advanced computational studies.

Keywords: Hückel theory; aza aromatic molecule; HuLiS software; geometry-based aromaticity; bond energy.

INTRODUCTION

Polycyclic π -conjugated carbon-based molecules have numerous potential applications in organic electronics; therefore, a detailed understanding of their fundamental properties is crucial.¹ Doping heteroatoms into carbon-based molecules is an effective strategy to adjust their physical and chemical properties of the material, thereby improving their performance in electronic, photonic, optoelectronic, and spintronic applications.²⁻¹¹ Nitrogen is the most commonly used dopant as it has a similar covalent radius as carbon while providing one extra electron. A fundamental property of heteroatom-doped carbon-based molecules is their stability with respect to the control of energy levels, which can be measured by the energy gap (E_{gap}).

Aromaticity is related to stability and E_{gap} , and it has been a central concept in organic chemistry for over a century.¹² Among the numerous aromaticity indices,^{13,14} a geometry-based aromaticity index is the most simple, successful, and widely used to quantitatively describe the π -electron delocalization in homo- and heteroatomic molecules. Starting from the harmonic oscillator model of aromaticity (HOMA),¹⁵⁻¹⁷ the model was developed for the harmonic oscillator model of electron delocalization (HOMED)^{18,19} and the harmonic oscillator model of heterocyclic electron delocalization (HOMHED).²⁰ These aromaticity indices use bond length data from molecular geometry, and the uniformity of π -electron distribution in the molecule is associated with the equalization of bond lengths. To calculate the aromaticity index, each of the three models uses some reference molecules or their related hybridizations to measure the optimal bond length from the single bond, R_s , and the double bond, R_d .

Hückel molecular orbital (HMO) theory is a well-known, simple theory, easily understood by undergraduate students, to predict E_{gap} and the behavior of the π -electron system.²¹⁻²³ The HMO

theory uses only the topology of the molecule, is independent of structural parameters, such as bond lengths and bond angles, and ignores the strain energy. For the heteroatoms, the Coulomb and resonance integral parameters can be adjusted according to the atom type and coordination number. These parameterizations are due to the different core energies of the heteroatom and the change in the effective electronegativity, compared with carbon, of the remaining non-bonded p orbitals at the center. Although the parameterizations are standardized in numerous chemistry and physics textbooks, the importance of distinguishing the Coulomb parameter of carbon atoms adjacent to heteroatoms is rarely emphasized. This is so particular for nitrogen-containing molecules, due to the large electronegativity of nitrogen.^{24,25} This parameterization should also depend on the molecule, which would require an additional parameter to measure the accuracy of the parameterization.

Pauling²⁶ established a formula relating bond length to bond order and an empirical rule for the relation between bond order and bond energy;²⁷ subsequently, Krygowski developed a model to estimate bond energy from bond length data.²⁸ Summation of the bond energy over all bonds of a cyclic molecule provides the ring energy content (REC), and summation over the entire molecule provides the molecule energy content (MEC).²⁹ Considering the CH bond energy, one may obtain the total molecular energy and compare it with the experimental data for the heat of formation.²⁸ Krygowski²⁸ and Cyrański³⁰ reported that the local and global aromaticity index of the HOMA correlates well with REC and MEC, with a higher mutual correlation for angular polyacenes compared with linear systems. However, the analyses so far are limited to benzenoid hydrocarbon molecules, leaving some questions regarding heteroatom molecules, including aza aromatic molecules.

This study applied a variation in the Hückel parameters of the aza aromatic molecules, acridine and phenazine. Previous theoretical studies have shown that the carbon atom adjacent to nitrogen should have a different Coulomb parameter owing to

*e-mail: im_sutjahja@itb.ac.id

the large electronegativity of nitrogen.^{24,25} However, the variation applied is not systematic, and generalization for its dependence on molecules is unclear.³¹ A further correction was performed based on the ring current model, which describes the flow of the π -electron system along the molecule's perimeter due to delocalization,^{32,33} as in the case of aromatic hydrocarbon molecules.^{34,35} The latter was implemented by assigning different resonance integral parameters for carbon-carbon atoms along the bridge of the molecule.³⁶ For this purpose, we used the HuLiS software,³⁷ which provides a facility for the proposed variations. The bond length data were further analyzed to predict the geometry-based aromaticity index based on the HOMA, HOMED, and HOMHED models. The results were used to examine the effect of each modified Hückel parameter on the molecular energy level and aromaticity of the two inequivalent rings. To estimate the bond energy from the bond length and its relation to the aromaticity index, the bond lengths of the single and double bonds were varied based on the values proposed in the three structure-based aromaticity models mentioned above.

Hückel molecular orbital theory

Parametrization of the Hamiltonian matrix element according to Hückel theory is:²¹⁻²³

$$H_{ij} = \langle p_i | H | p_j \rangle \begin{cases} \alpha, i=j \\ \beta, i-j = \pm 1 \end{cases} \quad (1)$$

where p_i is the $2p_z$ atomic orbital of the i^{th} order of the C atom; α is the Coulomb integral; and β is the resonance integral of the π -electron system. In addition, the overlap integral was diagonal.

$$S_{ij} = \delta_{ij} \quad (2)$$

For a molecule with a heteroatom, the Coulomb integral (h_x) and resonance integral (k_{xy}) of the π -electron system depends on the core energy and the change in the effective electronegativity of the remaining non-bonded p orbitals at the center. In this case, the values of α and β in Equation (1) can be written as^{21,22}

$$\alpha_x = \alpha + h_x |\beta| \quad (3a)$$

$$\beta_{xy} = k_{xy} |\beta| \quad (3b)$$

Table 1 lists the commonly accepted values of h_x and k_{xy} for C and N atoms.²²

Table 1. Values of Hückel parametrization²²

Element	h_x	k_{xy}
C	$h_C = 0.00$	$k_{CC} = 1.00$
N2*	$h_N = 0.51$	$k_{CN} = 1.02$
N3**	$h_N = 1.37$	$k_{CN} = 0.89$

*Dicoordinated. **Tricoordinated, planar geometry.

According to Hückel theory, the molecular orbital ψ is formed from atomic orbital p_i through a linear combination of atomic orbitals (LCAO) model, and the coefficients of atomic orbital $\{c_{ni}\}$ can be further used to obtain the π -electron bond order:

$$\rho_{ij} = v_n \sum_n c_{ni} c_{nj} \quad (4)$$

with v_n is the number of π -electrons occupying the corresponding energy level.

The energy gap is the difference between highest occupied molecular orbital (HOMO) level and the lowest unoccupied molecular orbital (LUMO) level,

$$E_{\text{gap}} = E_{\text{HOMO}} - E_{\text{LUMO}} \quad (5)$$

In addition, the delocalization energy is the difference between the total energies of the π -electron system and the simple isolated system.

$$E_{\text{deloc}} = E_{\text{total},\pi} - E_{\text{isolated}} \quad (6)$$

The isolated state of acridine ($C_{13}H_9N$) consists of six ethylene (C_2H_2) and one methane imine (CH_3N), whereas phenazine ($C_{12}H_8N_2$) consists of five ethylene and two methane imines.³⁸ The energies of one molecule of ethylene and methane imine are $2(\alpha + \beta)$ and $2\alpha + 2.61\beta$, respectively.

Bond order and bond length correlation

Pauling established a well-known formula relating the bond length $R(p)$ to its bond order p as²⁶

$$R(p) - R(1) = -c \ln p \quad (7)$$

where c is an empirical constant and $R(1)$ is the standard single bond length. The value of c can be calculated by taking the bond lengths for the typical single ($p = 1$) and double ($p = 2$) bonds as follows:

$$c = \frac{R(1) - R(2)}{\ln 2} \quad (8)$$

Using Equation (7), it is also possible to calculate the bond number, p , for any bond length, $R(p)$, as follows:

$$p = \exp\left(\frac{R(1) - R(p)}{c}\right) \quad (9)$$

Focusing to Huckel theory that deals with π -electron system, the bond length can be calculated from the π -electron bond order following Gordy's formula.^{39,40}

$$R = \sqrt{\frac{a}{b + N}} \quad (10)$$

where a and b are the modified Gordy values, equal to 7.33 and 2.09 for CC bonding, and 6.52 and 2.03 for CN bonding, respectively,⁴⁰ and $N = 1 + \rho_{ij}$ is the total bond order.³⁹

Geometry-based aromaticity index

The geometry-based aromaticity index of the HOMA¹³⁻¹⁷ is simple, successful, and widely used,⁴¹ both for homo- and heteroatomic systems. Subsequently, the HOMED^{18,19} and HOMHED were developed.²⁰ For each of these models, the bond length values for the single bond, R_s , and the double bond, R_d , were proposed according to the reference molecules.

In general the HOMA index can be calculated as^{13-17,42,43}

$$\text{HOMA} = 1 - \frac{1}{n} \sum_{i=1}^n \alpha_j (R_{o,j} - R_{j,i})^2 = 1 - \text{EN} - \text{GEO} \quad (11)$$

where n is the number of bonds taken into summation; and $R_{j,i}$ is the experimental or computed bond length of the system for a certain type of bond (j). In Equation (11), the summation is also held for

all types of bonds that are present in the ring of a molecule, that is, carbon–carbon (CC), carbon–nitrogen (CN), and nitrogen–nitrogen (NN) for the aza molecule. The optimal bond lengths R_o and α were calculated using the following formula.

$$R_o = \frac{R_s + wR_d}{1 + w} \quad (12)$$

$$\alpha = \frac{2}{(R_s - R_o)^2 + (R_d - R_o)^2} \quad (13)$$

where w is the ratio of the stretching force constants for pure single (R_s) and double (R_d) bonds, and the common value is equal to 2 for CC and CX bonds.⁴⁴ Table 2 presents the R_s , R_d , R_o , α , and c values for CC, CN, and NN bonds, and the reference molecule for each type of bond.

In Equation (11), it is clear that the decreased aromaticity in the π -electron system can be described by two different and independent mechanisms, namely, an increase in the bond length alternation (GEO) and an extension of the mean bond length (bond elongation) (EN); the latter is due to a decrease in the resonance energy. These two dearomatization terms, i.e., geometric GEO and energetic EN contributions, are calculated by transforming the bond order of CX or XY bonds. This is derived from Equation (9) considering the virtual CC bonds according to the Pauli formula (Equation (7)),

$$r(p) = 1.467 - 0.1702 \ln p \quad (14)$$

such that

$$\text{GEO} = \frac{257.7}{n} \sum_i (r_{av} - r_i)^2$$

$$\text{EN} = 257.7 (1.388 - r_{av})^2$$

where r_{av} represents the average value of r_i .

The HOMED index was proposed by Raczyńska *et al.*¹⁸ in 2010, primarily for molecules that contain heteroatoms. The HOMED index is formally the same as that of the HOMA, Equation (11) but differs for the reference molecules. Herein, quantum-chemical methods were used to estimate the bond lengths using simple saturated systems for single bonds and simple unsaturated systems for double bonds. The optimal bond length, R_o , was chosen from various simple molecules for which equalization of the bonds occurs. Table 3 presents the R_s , R_d , and R_o values for the HOMED calculations, along with the reference molecules.

The α calculation follows the following rules. For molecules with even numbers of bonds ($2i$), α can be calculated using Equation (13). In contrast, for molecules with odd numbers of bonds ($2i + 1$), α can be calculated using Equations (15) and (16), each of them for ($i + 1$) single bonds and (i) double bonds, and (i) single bonds, and ($i + 1$) double bonds.

$$\alpha = \frac{2i + 1}{(i + 1)(R_o - R_s)^2 + i(R_o - R_d)^2} \quad (15)$$

$$\alpha = \frac{2i + 1}{i(R_o - R_s)^2 + (i + 1)(R_o - R_d)^2} \quad (16)$$

The HOMHED model proposed by Frizzo *et al.*²⁰ in 2012 is based on the average experimental (X-ray diffraction and neutron diffraction) data of several reference molecules. Table 4 presents the R_s , R_d , R_o , and α values for the HOMHED calculation, along with the hybridization of the reference molecules for a particular type of bonding. The HOMHED index was calculated using Equation (11).

Table 2. Values of R_s , R_d , R_o , α and c for the HOMA index along with reference molecules^{15,43}

Type of bond	R_s (Å)	R_d (Å)	R_o (Å)	α	c	Reference molecule
CC	1.467	1.349	1.388	257.7	0.1702	1,3-butadiene, CH ₂ =CH–CH=CH ₂
CN	1.465	1.269	1.334	93.52	0.2828	Methylamine, H ₂ N–CH ₃ and methylene imine, HN=CH ₂
NN	1.420	1.254	1.309	130.33	0.2395	(CH ₃) ₂ C=N–N(CH ₃) ₂ and H ₃ C–N=N–CH ₃

Table 3. Values of R_s , R_d , and R_o for the HOMED index along with the reference molecules^{18,19}


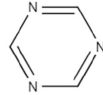
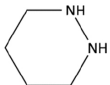
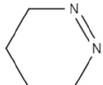
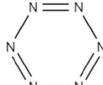
Type of bond	R_s (Å)	Molecule reference	R_d (Å)	Molecule reference	R_o (Å)	Reference molecule
CC	1.5300	H ₃ C–CH ₃	1.3288	H ₂ C=CH ₂	1.3943	
CN	1.4658	H ₃ C–NH ₂	1.2670	H ₂ C=NH	1.3342	
NN	1.4742		1.2348		1.3193	

Table 4. Values of R_s , R_d , R_o , and α for the HOMHED index along with the hybridization of the reference molecules²⁰

Type of bond	R_s (Å)	R_d (Å)	R_o (Å)	α	Hybridization of the reference molecules
CC	1.530	1.316	1.387	78.6	C _{sp³} –C _{sp³} ; C _{sp²} –C _{sp²}
CN	1.474	1.271	1.339	87.4	C–N _{sp³}
NN	1.454	1.240	1.311	78.6	N _{sp³} –N _{sp³} ; C–N=N–C

Bond energy from bond length

Bond energy is related to geometry-based aromaticity indices and is estimated from the bond length. For benzenoid hydrocarbon molecules, Krygowsky *et al.*²⁸ has developed a model that relates the bond energy, $E(i)$, calculated directly from the bond length as:

$$E(i) = E(1) \exp[\alpha' \{R(1) - R(i)\}] \quad (17)$$

where $R(1)$ and $E(1)$ are the bond lengths of a single bond and its associated energy, respectively; $R(i)$ and $E(i)$ are the investigated bond lengths in the molecule and its related energy, respectively; and α' is an empirical constant that can be calculated according to the reference bond lengths and bond energies that correspond to the single and double bonds. Generalization of the above formula to aza aromatic molecules was performed by considering the CN and NN bonds in addition to CC bonding. The REC can be obtained by summing $E(i)$ for all bonds in a ring of the molecule, as follows.

$$\text{REC} = \sum_{i=1}^n (E(i)) \quad (18)$$

whereas the MEC can be obtained by summing over the molecule. Considering the carbon and hydrogen bonds in the molecule, one can obtain the total bond energy of the molecule:

$$E_{\text{molecule}} = E_{\text{CH}} + E(1) \sum_{i=1}^n \exp[\alpha' \{R(1) - R(i)\}] \quad (19)$$

This value can be compared with the experimental data for the heat of formation from atoms (HtFfA),²⁸

$$\text{HtFfA} = \Delta H_{f,\text{molecule}} + n_k \sum_k H_{A,k} \quad (20)$$

where $\Delta H_{f,\text{molecule}}$ is the heat of formation of the corresponding molecule; and H_A is the heat of atomization; additionally, summation (k) is performed for all atoms that make up the molecule.

METHODS

HuLiS software

HuLiS³⁷ is a software package for molecular electronic structure calculations based on the Hückel method. Figure 1 shows the HuLiS software interface. The input parameter used to solve the Hamiltonian system is the molecular drawing. This software allows for a change in the Coulomb integral of any atom (α) or resonance integral (β) by clicking on a certain atom or bonding.

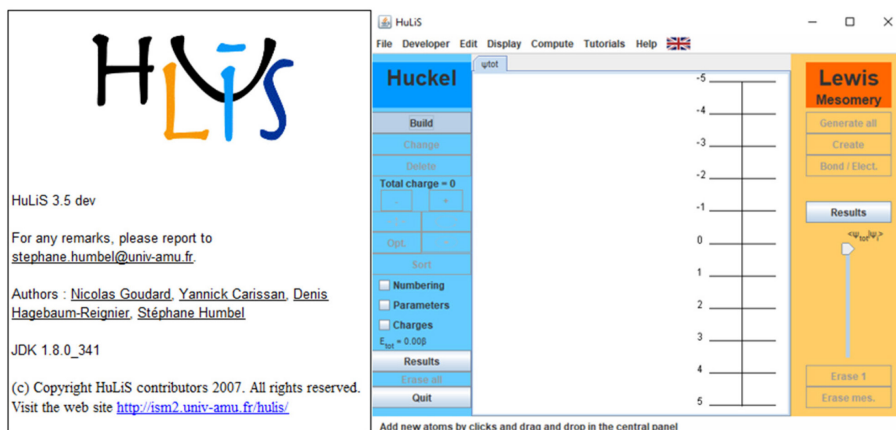


Figure 1. HuLiS software interface

The output consists of the energy level and the coefficients of the linear combination of molecular orbitals. Additionally, this software can display the electron distribution profile for each energy level.

Parametrization of Hückel parameters

For various N-doped molecules of pyridine, quinoline, isoquinoline, and acridine, Longuet-Higgins and Coulson in 1946²⁴ proposed the same correction to the Coulomb integrals of nitrogen and carbon atoms that directly bonded to nitrogen, whereas Dasgupta in 1964²⁵ proposed different parameter values that depend on the molecular type, as presented in Table 5. In this table, α is the Coulomb integral for all other carbon atoms and β is the resonance integral of the CC bonding.

Table 5. Different Coulomb and resonance parameters of aza aromatic molecules from previous studies^{24,25}

Molecule	α_N	α_{CN}	Reference
Pyridine	$\alpha + 2\beta$	$\alpha + 0.25\beta$	24
	$\alpha + 0.2\beta$	$\alpha + 0.025\beta$	25
Quinoline	$\alpha + 0.2\beta$		25
Iso-Quinoline	$\alpha + 0.2\beta$		25
Acridine	$\alpha + 2\beta$	$\alpha + 0.25\beta$	24
	$\alpha + 0.66\beta$	$\alpha + 0.0825\beta$	25

The data presented in Table 5 reveal a significant difference in the parameter values, whereas the commonly accepted values are listed in Table 1, without the need to give the difference for the carbon atom close to nitrogen.

Herein, we performed a systematic study for the parametrization of the Hückel parameters of acridine and phenazine, which consist of the Coulomb integral of carbon adjacent to nitrogen (α_{CN}) and the resonance integral for CC bonding (β_{CC}) along the bridge of the molecule, expressed in terms of resonance energy,³⁶

$$\beta_{CC} = \gamma |\beta| \quad (21)$$

The values of α_{CN} are 0, 0.025, 0.050, 0.075, 0.0825, 0.100, and 0.250; and $1.0 \leq \gamma \leq 1.5$ with steps of 0.1.

Bond energy and heat of atomization

To compare the total bond energy and heat of formation from atoms, Table 6 lists the experimental data for the heat of atomization

of C, H, and N from the gas phase and the bond dissociation energies of C–H, C–C, C=C, C–N, and C=N.⁴⁵ Table 7 lists the experimental data for the enthalpy of formation of the investigated molecules.

Table 6. Heat of atomization, bond dissociation energy⁴⁵

ΔH_f (kcal mol ⁻¹)		E_b (kcal mol ⁻¹)	
C(g)	171.2	C–H	98.3
H(g)	52.1	C–C	82.6
N(g)	112.9	C=C	144.0
		C–N	72.8
		C=N	147.0

Table 7. Enthalpy of formation of molecule

Molecule	Formula	ΔH_f (kJ mol ⁻¹)	ΔH_f (kcal mol ⁻¹)	Reference
Benzene (l)	C ₆ H ₆	49	11.70	46
Naphthalene (s)	C ₁₀ H ₈	78	18.63	46
Anthracene (s)	C ₁₄ H ₁₀	127	30.33	46
Phenanthrene (s)	C ₁₄ H ₁₀	110	26.27	46
Pyridine (l)	C ₅ H ₅ N	100.02	23.89	47
Acridine (g)	C ₁₃ H ₉ N	273.9	65.42	48,49
Phenazine (g)	C ₁₂ H ₈ N ₂	338.3	80.80	50

RESULTS AND DISCUSSION

The results of Hückel method

The molecular structures of acridine and phenazine are shown in Figure 2. The direct application of the Hückel method to acridine and phenazine by applying the Coulomb integral and resonance integral parameters listed in Table 1 gave the energy level diagram shown in the above panel of Figure 2. This figure shows that for both molecules, the energy levels of the HOMO-1 and LUMO+1 states consist of degenerate states. However, group theory predicted no degeneracy for the two molecules in the C_{2v} or D_{2h} point groups.⁵¹⁻⁵³

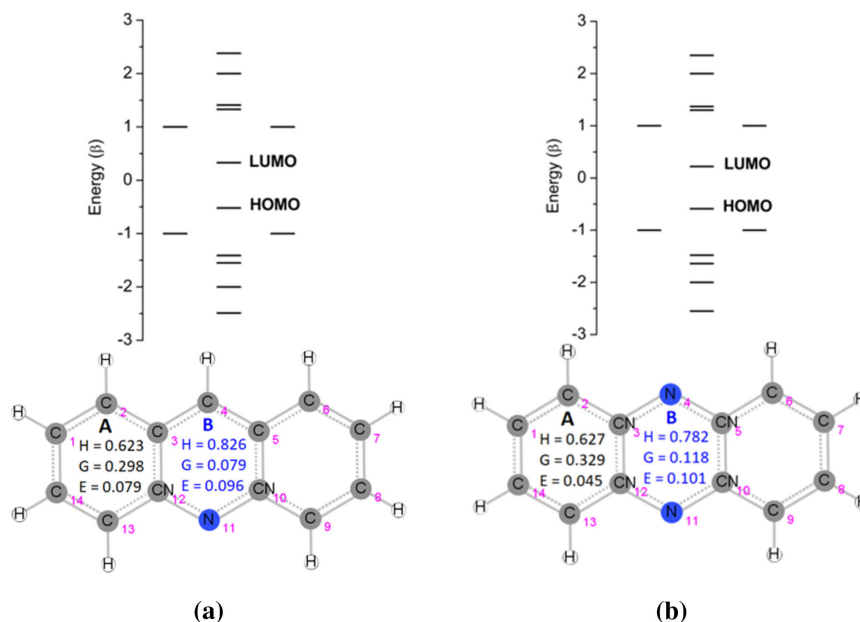


Figure 2. Molecular structure with atomic numbering and energy level diagram of (a) acridine and (b) phenazine. The numbers in the rings represent the index values of HOMA (H), GEO (G), and EN (E) calculated from experimental geometric data^{53,54}

As shown in Figure 2, the aromaticity indices for the two non-equivalent rings from the previous structural data of acridine⁵⁴ and phenazine⁵³ clearly demonstrate that the ring containing the nitrogen atom (B) is more aromatic than the benzene ring (A).^{55,56} Furthermore, for ring-B of the two molecules, the index value of EN is comparable to GEO. We observe that, particularly for acridine, this variation in the aromaticity index cannot be qualitatively obtained from the direct application of the Hückel method.

Correction to Hückel parameters

Figure 3 illustrates the results of the HOMA aromaticity index of the two non-equivalent molecular rings of (a) acridine and (b) phenazine for the variation of α_{CN} (i) and β_{CC} (ii). Evidently, different models of the aromaticity index (HOMED and HOMHED) exhibited similar profiles, although with different absolute values. As shown in this figure, the standard deviation of the bond length was compared with the corresponding values from Phillips⁵⁴ for acridine and Wozniak *et al.*⁵³ for phenazine.

Evidently from Figure 3(i), upon varying α_{CN} , the aromaticity index of the ring-A is smaller than the aromaticity index of ring-B that contains nitrogen for $\alpha_{CN} = 0.1$ for acridine, whereas for phenazine, it occurred for all values of α_{CN} and a minimum in the standard deviation value of the bond length was observed for $\alpha_{CN} = 0.1$. However, using different parameters for carbon atoms close to nitrogen removed the degeneracy in the energy levels of acridine and phenazine, which is in good agreement with a previous semi-empirical self-consistent field study.²⁴ When varying β_{CC} , a minimum in the standard deviation value of bond length occurred at $\beta_{CC} = 1.1$ for acridine and 1.2 for phenazine. Thus, we concluded that the best modified Hückel parameters for α_{CN} and β_{CC} are 0.1 and 1.1 for acridine and 0.1 and 1.2 for phenazine, respectively. In addition, set values of aromaticity indices for acridine are {H = 0.805, G = 0.088, E = 0.107} for ring-A and {H = 0.837, G = 0.044, E = 0.119} for ring-B. The same indices for phenazine are {H = 0.791, G = 0.104, E = 0.105} for ring-A and {H = 0.883, G = 0.057, E = 0.060} for ring-B. By modifying the Hückel parameters, it can be seen that the aromaticity indices of the two molecules qualitatively agree with the experimental results presented previously.

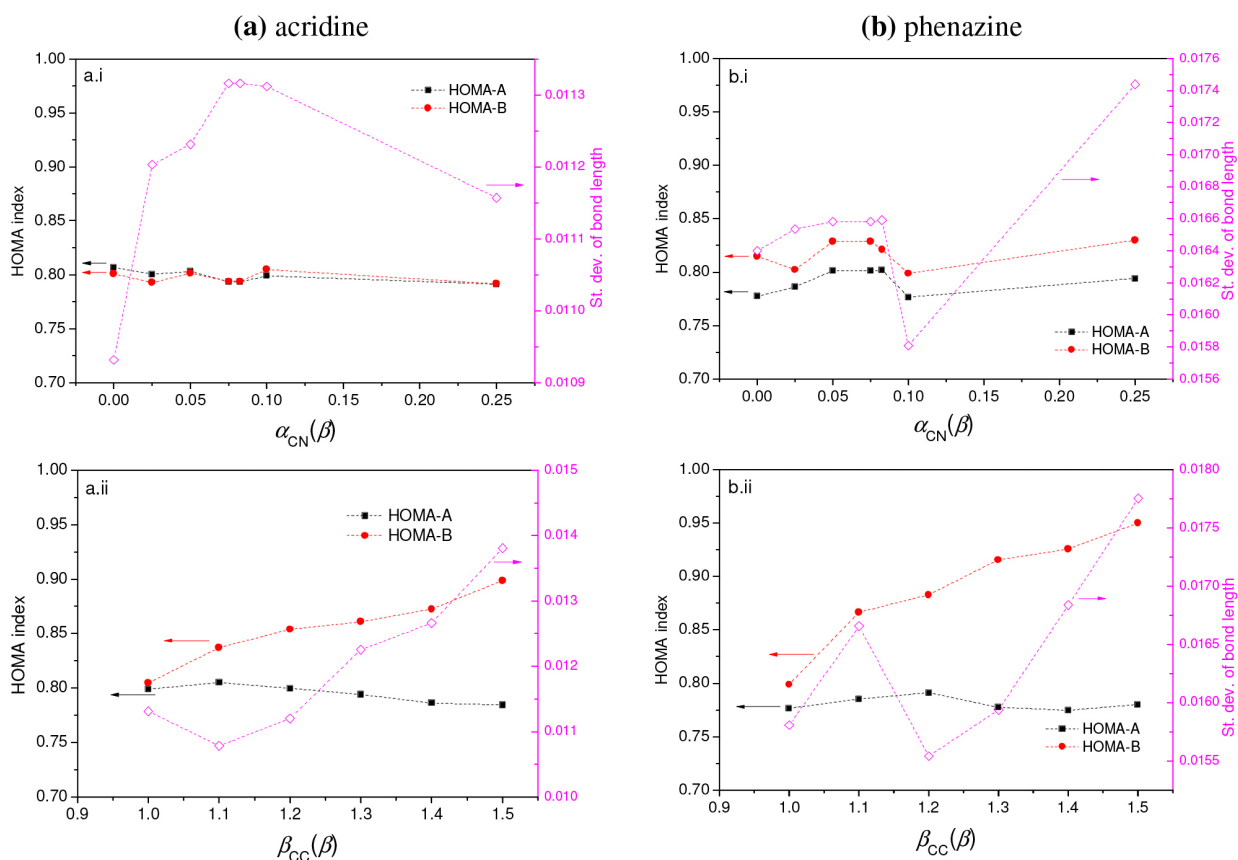


Figure 3. Results of aromaticity index of HOMA of the two non-equivalent rings (A and B) of (a) acridine and (b) phenazine, for the variation of (i) α_{CN} (for $\beta_{CC} = 1.0$) and (ii) β_{CC} (for $\alpha_{CN} = 0.1$). For all graphs, the right axis shows the standard deviation of bond length

Bond length and molecular orbital description

Figure 4 shows the calculated bond lengths for some unique bonds of the two molecules for the best parameters compared with previous theoretical and experimental studies. To study the effect of nitrogen, we plotted anthracene data from a previous study using the same method with the best correction to the Hückel parameters.³⁶ Figure 4 shows that the results are in good agreement with previous studies. For the best corrected Hückel parameters, the standard deviation values of the bond length compared with the experimental data^{53,54} were 1.08 % for acridine and 1.55 % for phenazine.

Figure 4 shows that for both molecules the CC bond distance of the benzene ring (ring A) was 1.34–1.44 Å, whereas the CN distance

of the nitrogen-containing ring (ring B) was approximately 1.34 Å, both consistent with a delocalized scheme. The bonding properties of the outer rings of acridine and phenazine were similar to each other and to those of anthracene, differing only in the middle ring. This result is in good agreement with previous studies^{51,57} and is supported by the fact that the force constants of the outer rings of the three molecules are similar, differing in the middle ring due to the presence of the nitrogen atom.⁵⁷

Further, we noted a mistake in the bonding labels in Figure 6(a) in Sudarso *et al.*³⁶ with reference to the numbering of the carbon atoms of anthracene in Figure 2(a) of the same reference; the correct bonding labels should be 1-2, 1-11, 9-11, 2-3, 11-12.

The molecular energy level diagram for the best modified

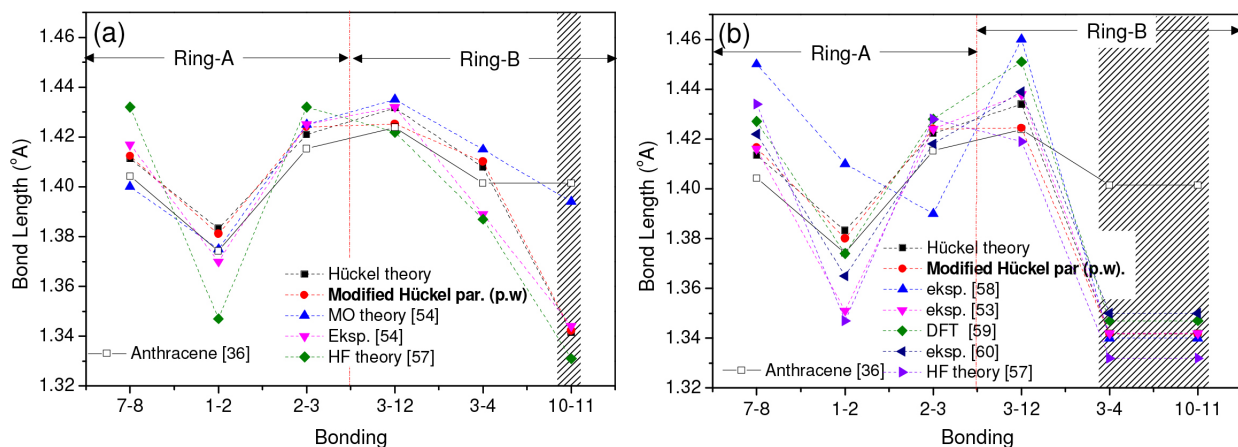


Figure 4. Bond length of (a) acridine and (b) phenazine from the present work with the best result for the modified Hückel parameters, compared with the data for anthracene³⁶ and experimental and computational data from previous studies.^{53,54,57-60} Shading denotes CN bonding

Hückel parameter and the associated HOMO and LUMO obtained from LCAO model are summarized in Table 8 for both acridine and phenazine. Data for anthracene were obtained from our previous study.³⁶

Evident from the molecular energy level diagram, degeneracy in the energy levels of acridine and phenazine was removed, which is consistent with a previous semi-empirical self-consistent field-LCAO-MO study.²⁴ The HOMO and LUMO plots obtained resembled those obtained from the density functional theory (DFT) studies of Adad⁶¹ for acridine and Zendaoui⁵⁹ for phenazine. The HOMO and LUMO plots for acridine and phenazine were similar to those of anthracene. In particular, the HOMO is localized primarily on the two C6 rings but extends to a certain degree to the central ring. In contrast, the LUMO is localized primarily on the central ring and presents a non-negligible contribution from the C6 rings. For acridine and phenazine, the essential contributor of the central ring is from the nitrogen atoms.

Table 9 compares some of the energy characteristics of the two studied molecules with those of anthracene, compared with previous experimental and advanced calculation studies. This correction shows that the HOMO-LUMO gap energy was 0.84β for acridine and 0.77β for phenazine. In addition, the delocalization energy was 5.72β for acridine and 6.07β for phenazine. The higher gap energy of acridine relative to phenazine agrees with previous experiments and advanced computational studies. Compared with anthracene, the trend of the gap energy was consistent with the experimental optical band-gap data, and the gap energy decreased with increasing nitrogen to carbon ratio, which is in good agreement with a previous study.⁶² The delocalization energy of phenazine was found to be larger than

acridine, which is in good agreement with the increased molecular stability when increasing the number of nitrogen atoms, but still smaller than the parent molecule anthracene.

Based on the result of the HOMO energy, with $\beta < 0$, one might expect a substantial shift to higher ionization energies from anthracene to acridine and phenazine, which is consistent with previous computational studies.^{67,68} In contrast, the opposite trend was observed for the LUMO energy.

Bond energy and heat of formation from atoms

Figure 5 shows a comparison of the total molecular energy with the experimental HtFfA for various benzenoid hydrocarbons (a) and aza aromatic molecules (b). For the benzenoid hydrocarbons anthracene and phenanthrene, we used the best modified Hückel parameters, as reported previously.³⁶ For both groups of molecules, increasing the number of rings increased HtFfA, and the HtFfA value of the angular molecule, phenanthrene was larger than that of the linear molecule, anthracene. For aza aromatic molecules, increasing the number of nitrogen atoms from acridine to phenazine decreased HtFfA. In addition, the dependence of HtFfA on the number of ring molecules and nitrogen atoms is shown by the smaller corresponding values of pyridine compared to those of benzene and the larger corresponding values of acridine compared with those of anthracene.

In general, the variation in the total molecular energy related to the three aromaticity indices followed the experimental HtFfA value. However, a smaller deviation was observed for the bond energies derived from the bond lengths based on the HOMED,

Table 8. Energy level diagram and plots of HOMO and LUMO of acridine and phenazine from the present work compared with those of anthracene. Different colors of red and grey circles indicate the positive and negative coefficients of linear combinations, respectively

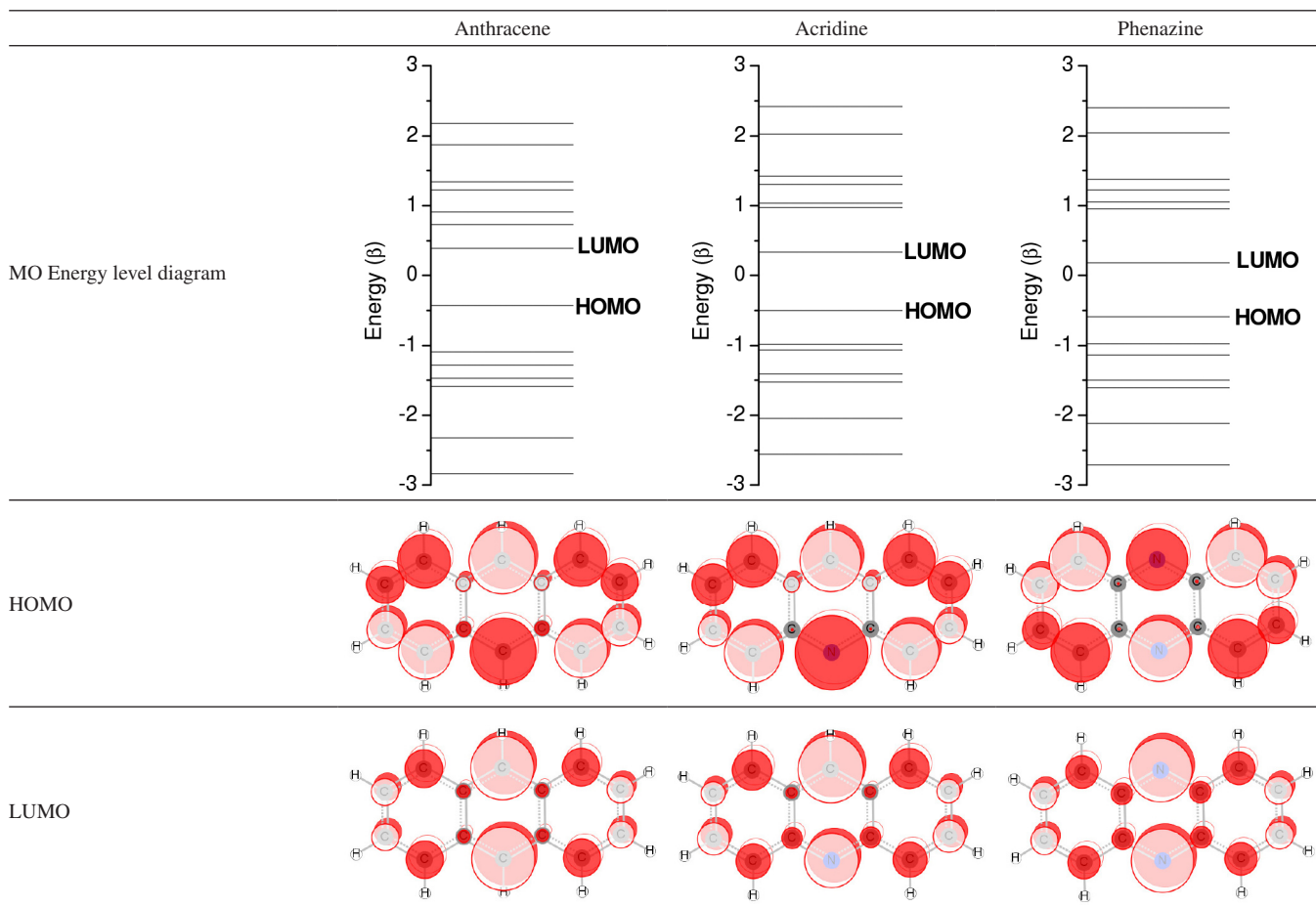
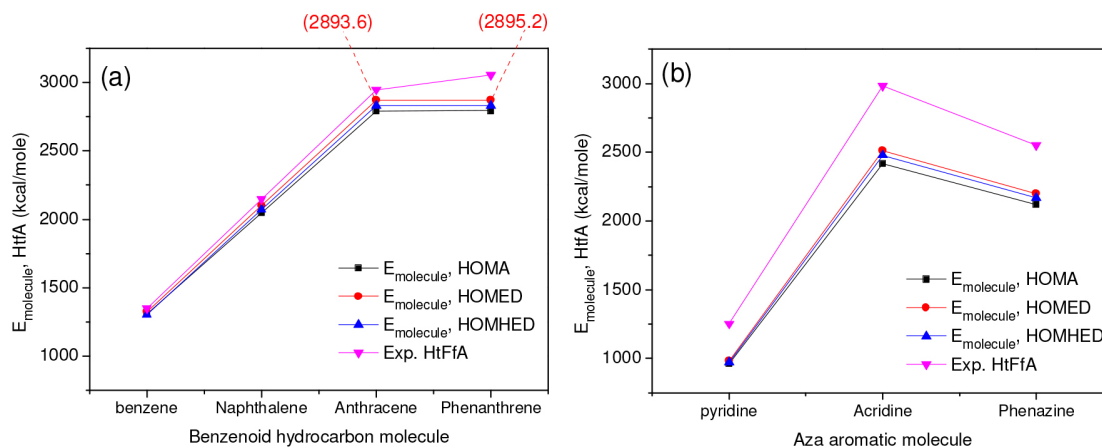


Table 9. HOMO–LUMO gap energy, delocalization energy, HOMO and LUMO energies, and optical band gap of phenazine and acridine from the present work (p.w) and previous experimental and advanced calculation studies, compared with those of anthracene.

Molecule	HOMO–LUMO gap energy	E_{deloc}	E_{HOMO}	E_{LUMO}	HOMO–LUMO gap energy (eV)	$E_{\text{g,opt}}$ (eV)
Anthracene	$0.82\beta^{36}$	$8.08\beta^{36}$	$0.43\beta^{36}$	$-0.39\beta^{36}$	3.58^{63}	3.20^{*63}
Acridine	0.84β (p.w)	5.72β (p.w)	0.52β (p.w)	-0.32β (p.w)	3.7^{64} 3.701^{61}	3.22^{*65}
Phenazine	0.77β (p.w)	6.07β (p.w)	0.59β (p.w)	-0.18β (p.w)	2.37^{59}	3.07^{66}

*Estimated from the absorption spectra by determining the wavelength of absorption onset and converting it from nm to eV.⁶²

**Figure 5.** Total molecular energy based on HOMA, HOMED and HOMHED calculations compared with the experimental HtFfA for (a) benzenoid hydrocarbon and (b) aza aromatic molecules. The numbers on (a) are E_{molecule} of anthracene and phenanthrene calculated based on HOMED

followed by those derived from the HOMHED and HOMA. In particular, all models predicted a larger total molecular energy value for phenanthrene compared with anthracene, which is in agreement with the experimental HtFfA. Thus, the modified Hückel parameters yielded total molecular energy values that matched the experimental data. Compared with benzenoid hydrocarbon molecules, a larger deviation between the calculated total energy molecular and experimental HtFfA values was found for the aza aromatic molecules.

To further correlate the bond energy with the aromaticity index, Table 10 presents the corresponding aromaticity HOMED index with the REC divided by the number of CC and CN bonds (n).

Evidently, aromaticity varied with an increase in the number of rings and the number of nitrogen atoms in the molecule. For anthracene, the aromaticity of the central benzene ring was higher than that of the outer benzene ring. The opposite trend was observed for phenanthrene, which is in good agreement with our previous study³⁶ using the HOMA aromaticity index. With an increased number of rings, the aromaticity index generally decreased, as reported previously^{30,55}. Upon replacement of carbon with nitrogen, the aromaticity index of nitrogen-containing rings increased (for example, 0.994 for acridine as compared with 0.972 for anthracene), whereas the aromaticity index of the benzene ring decreased (0.952 for acridine as compared with 0.961 for anthracene). This result is consistent with previous studies.^{55,56} For acridine and phenazine, the aromaticity index of the nitrogen-containing ring was higher than that of the benzene ring, which was consistent with previous studies using geometric experimental data.^{55,56} However, the smaller aromaticity index for the benzene- and nitrogen-containing rings in phenazine compared with those of acridine indicates that further increase in the number of nitrogen atoms decreased the aromaticity index.

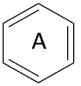
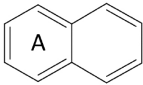
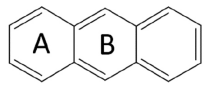
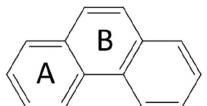
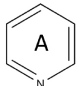
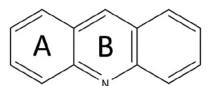
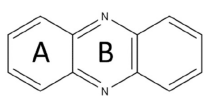
Interestingly, for both groups of molecules, the variation in REC/ n from the present study generally followed the corresponding values from experimental geometry data.³⁰ The results of the present study

show that the REC/ n value generally decreased as the number of rings increased. In addition, upon replacing carbon with nitrogen, the REC/ n value generally decreased for both single-ring molecules and for benzene- and nitrogen-containing rings. The results presented in this study should be supported by further analysis based on advanced calculations studies, in particular, studies on the relationship between aromaticity and the number of nitrogen atoms and NN bonding, as well as the topological environment of the ring.^{32,55}

CONCLUSIONS

This study presented a correction to the Hückel parameters of the aza aromatic molecules acridine and phenazine. The parameter correction consists of the Coulomb integral of the carbon atom adjacent to nitrogen (α_{CN}) and the resonance integral of the carbon–carbon atoms (β_{CC}). The latter is based on the ring current model, which describes the delocalization of π -electrons along the perimeter of the molecule. The calculation was performed using HuLiS software. The resulting bond order was transformed into a bond length based on Gordy's formula with modified Gordy values. The validity of the results was examined using the structurally based aromaticity indices of the HOMA, HOMED, and HOMHED. For the three aromaticity indices, the experimental data of the two molecules revealed that the nitrogen-containing ring is more aromatic than the benzene ring. Additionally, both α_{CN} and β_{CC} parameters were found to be responsible for the excessive degeneracy in the molecular orbitals. The best values of α_{CN} and β_{CC} were 0.1 and 1.1 for acridine and 0.1 and 1.2 for phenazine, respectively. Comparison of the calculated bond lengths with previous experimental and advanced calculation studies revealed a delocalized scheme of CC and CN bonding. Compared with anthracene, the bonding properties of the outer rings of acridine and phenazine were similar to each other and also similar to anthracene, differing only in the middle ring owing to the presence of nitrogen

Table 10. Aromaticity indices of HOMED and REC/n for the individual rings. The values in the parentheses are calculated from experimental geometry data listed in the reference

Group	Molecule	Molecule	Ring	HOMED index	REC/n	Reference
Benzenoid hydrocarbon	Benzene		A	0.997	122.3 (118.8)	69
	Naphthalene*		A	0.967	119.1 (116.6)	70
	Anthracene		A	0.961	118.1 (116.7)	71
			B	0.972	115.5 (115.3)	
	Phenanthrene		A	0.986	119.5 (117.0)	71
B			0.922	114.9 (111.3)		
Aza aromatic	Pyridine		A	0.999	118.7 (113.8)	72
	Acridine		A	0.952	115.7 (116.1)	54
			B	0.994	112.7 (114.1)	
	Phenazine		A	0.948	115.8 (118.4)	53
B			0.970	112.1 (110.8)		

*The modified Hückel parameters of $\alpha = 0.5$, $\gamma = 1.5$.

atoms. The HOMO-LUMO energy gap was 0.84β for acridine and 0.77β for phenazine, which is in good agreement with the smaller energy gap of phenazine compared to acridine from previous DFT and experimental studies. The delocalization energy of phenazine (6.07β) was larger than that of acridine (5.72β), which is in good agreement with the trend of increasing molecular stability with an increasing number of nitrogen atoms, but they are still smaller than anthracene.

To further validate the aromaticity index, we calculated the molecular bond energy from the bond length for several benzenoid hydrocarbons and aza aromatic molecules, including acridine and phenazine. Considering the energy related to the CH bond, the total molecular energy data were compared with the experimental data for the heat of formation from atoms (HtFfA). The comparison revealed that in general, modified Hückel parameters with calculated bond energies derived from the three aromaticity indices based on each single and double bond length as the reference resemble the experimental HtFfA. The smallest deviation was observed for the bond energy derived from the HOMED model. However, a larger difference between the two values for aza aromatic molecules may indicate some limitations of the existing model. A correlation study between the HOMED index and REC divided by the number of CC and CN bonds revealed a different role between the number of rings and nitrogen atoms. Remarkably, the results from the simple Hückel theory with modified parameters can resemble the experimental results, from the viewpoints of the aromaticity index and energy related to the bond length. However, advanced computational studies are needed to confirm these results and to achieve a better understanding of the relationship between the aromaticity index and molecular energy from bond length and the bonding properties of a particular molecule.

ACKNOWLEDGEMENTS

This study is the output of the P2MI ITB 2023 research scheme. It is dedicated to the late Professor Pantur Silaban for his memorable contributions to theoretical physics at the Physics Department, Faculty of Mathematics and Natural Sciences, Institut Teknologi Bandung.

REFERENCES

- Kubozono, Y.; *Physics and Chemistry of Carbon-Based Materials*, 1st ed.; Springer: Singapore, 2019.
- Anthony, J. E.; *Chem. Rev.* **2006**, *106*, 5028. [Crossref]
- Mei, J.; Diao, Y.; Appleton, A. L.; Fang, L.; Bao, Z.; *J. Am. Chem. Soc.* **2013**, *135*, 6724. [Crossref]
- Miao, Q.; *Polycyclic Arenes and Heteroarenes: Synthesis, Properties, and Applications*, 1st ed.; Wiley-VCH: Weinheim, 2015.
- Yutomo, E. B.; Noor, F. A.; Winata, T.; *RSC Adv.* **2021**, *11*, 18371. [Crossref]
- Ostroverkhova, O.; *Chem. Rev.* **2016**, *116*, 13279. [Crossref]
- Ghosh, S.; Barg, S.; Jeong, S. M.; Ostrikov, K. (Ken); *Adv. Energy Mater.* **2020**, *10*, 2001239. [Crossref]
- Woo, J.; Lim, J. S.; Kim, J. H.; Joo, S. H.; *Chem. Commun.* **2021**, *57*, 7350. [Crossref]
- Wang, X.-Y.; Yao, X.; Narita, A.; Müllen, K.; *Acc. Chem. Res.* **2019**, *52*, 2491. [Crossref]
- Zhang, J.; Xia, Z.; Dai, L.; *Sci. Adv.* **2015**, *1*, 1. [Crossref]
- Irham, M. A.; Anrokhi, M. S.; Anggraini, Y.; Sutjahja, I. M.; *Quim. Nova* **2021**, *44*, 1204. [Crossref]
- Minkin, V. I.; Glukhovtsev, M. N.; Simkin, B. Y.; *Aromaticity and*

- Antiaromaticity: Electronic and Structural Aspects*, 1st ed.; Wiley-Interscience: New York, 1994.
13. Szatyłowicz, H.; Wieczorkiewicz, P. A.; Krygowski, T. M.; *Sci* **2022**, *4*, 24. [Crossref]
14. Fernandez, I.; *Aromaticity (Modern Computational Methods and Applications)*, 1st ed.; Elsevier: Amsterdam, 2021.
15. Krygowski, T. M.; Szatyłowicz, H.; *ChemTexts* **2015**, *1*, 12. [Crossref]
16. Krygowski, T. M.; *J. Chem. Inf. Comput. Sci.* **1993**, *33*, 70. [Crossref]
17. Krygowski, T. M.; Szatyłowicz, H.; Stasyuk, O. A.; Dominikowska, J.; Palusiak, M.; *Chem. Rev.* **2014**, *114*, 6383. [Crossref]
18. Raczyńska, E. D.; Hallman, M.; Kolczyńska, K.; Stępniewski, T. M.; *Symmetry* **2010**, *2*, 1485. [Crossref]
19. Raczyńska, E. D.; *Symmetry* **2019**, *11*, 146. [Crossref]
20. Frizzo, C. P.; Martins, M. A. P.; *Struct. Chem.* **2012**, *23*, 375. [Crossref]
21. Yates, K.; *Hückel Molecular Orbital Theory*; Academic Press: New York, 2012.
22. Rauk, A.; *Orbital Interaction Theory of Organic Chemistry*, 2nd ed.; John Wiley & Sons: New York, 2001.
23. Tjia, M. O.; Sutjahja, I. M.; *Orbital Kuantum - Pengantar Teori dan Contoh Aplikasinya*; Karya Putra Darwati Bandung: Bandung, 2012.
24. Longuet-Higgins, H. C.; Coulson, C. A.; *Trans. Faraday Soc.* **1947**, *43*, 87. [Crossref]
25. Dasgupta, M.; *Proc. Indian Natl. Sci. Acad.* **1965**, *31*, 413. [Link] accessed in January 5, 2023
26. Pauling, L.; *J. Am. Chem. Soc.* **1947**, *69*, 542. [Crossref]
27. Johnston, H. S.; Parr, C.; *J. Am. Chem. Soc.* **1963**, *85*, 2544. [Crossref]
28. Krygowski, T. M.; Ciesielski, A.; Bird, C. W.; Kotschy, A.; *J. Chem. Inf. Comput. Sci.* **1995**, *35*, 203. [Crossref]
29. Krygowski, T. M.; Cyrański, M. K.; *Theor. Comput. Chem.* **1998**, *5*, 153. [Crossref]
30. Cyrański, M. K.; Stępień, B. T.; Krygowski, T. M.; *Tetrahedron* **2000**, *56*, 9663. [Crossref]
31. Sevenster, A. J. L.; Tabner, B. J.; *Magn. Reson. Chem.* **1984**, *22*, 521. [Crossref]
32. Abraham, R. J.; Reid, M.; *J. Chem. Soc., Perkin Trans. 2* **2002**, *2*, 1081. [Crossref]
33. Najmidin, K.; Kerim, A.; Abdirishit, P.; Kalam, H.; Tawar, T.; *J. Mol. Model.* **2013**, *19*, 3529. [Crossref]
34. Steiner, E.; Fowler, P. W.; *Int. J. Quantum Chem.* **1996**, *60*, 609. [Crossref]
35. Cuesta, I. G.; De Merás, A. S.; Pelloni, S.; Lazzeretti, P.; *J. Comput. Chem.* **2008**, *30*, 551. [Crossref]
36. Sudarso, Y. P. D.; Maulana, A. L.; Soehiani, A.; Sutjahja, I. M.; *Quim. Nova* **2022**, *45*, 742. [Crossref]
37. Carissan, Y.; Hagebaum-Reignier, D.; Goudard N.; Humbel S.; *J. Phys. Chem. A* **2008**, *112*, 13256. [Crossref]
38. Dascălu, D.; Isac, D.; Pahomi, A.; Isvoran, A.; *Rom. J. Biophys.* **2018**, *28*, 59. [Crossref]
39. Gordy, W.; *J. Chem. Phys.* **1947**, *15*, 305. [Crossref]
40. Paolini, J. P.; *J. Comput. Chem.* **1990**, *11*, 1160. [Crossref]
41. Kwapisz, J. H.; Stolarczyk, L. Z.; *Struct. Chem.* **2021**, *32*, 1393. [Crossref]
42. Cyrański, M. K.; Krygowski, T. M.; *Tetrahedron* **1999**, *55*, 6205. [Crossref]
43. Krygowski, T. M.; Cyrański, M.; *Tetrahedron* **1996**, *52*, 10255. [Crossref]
44. Kruzewski, J.; Krygowski, T. M.; *Tetrahedron Lett.* **1972**, *13*, 3839. [Crossref]
45. Huheey, J. E.; Keiter, E. A.; Keiter, R. L.; *Inorganic Chemistry: Principles of Structure and Reactivity*, 4th ed.; HarperCollins College: New York, 1993.
46. Roux, M. V.; Temprado, M.; *J. Phys. Chem. Ref. Data* **2008**, *37*, 1855. [Crossref]
47. Hubbard, W. N.; Frow, F. R.; Waddington, G.; *J. Phys. Chem.* **1961**, *65*, 1326. [Crossref]
48. National Institute of Standards and Technology (NIST); *Standard Reference Database 69: Acridine*; NIST Chemistry WebBook, 2021. [Link] accessed in January 5, 2023
49. Steele, W. V.; Chirico, R. D.; Hossenlopp, I. A.; Nguyen, A.; Smith, N. K.; Gammon, B. E.; *J. Chem. Thermodyn.* **1989**, *21*, 81. [Crossref]
50. National Institute of Standards and Technology (NIST); *Standard Reference Database 69: Phenazine*; NIST Chemistry WebBook, 2021. [Link] accessed in January 5, 2023
51. Fu, A.; Du, D.; Zhou, Z.; *Spectrochim. Acta, Part A* **2003**, *59*, 245. [Crossref]
52. Li, W. H.; Li, X. Y.; Yu, N. T.; *Chem. Phys. Lett.* **2000**, *327*, 153. [Crossref]
53. Woźniak, K.; Kariuki, B.; Jones, W.; *Acta Crystallogr., Sect. C: Struct. Chem.* **1991**, *47*, 1113. [Crossref]
54. Phillips, D. C.; *Acta Crystallogr.* **1956**, *9*, 237. [Crossref]
55. Krygowski, T. M.; Cyrański, M. K.; *Chem. Rev.* **2001**, *101*, 1385. [Crossref]
56. Cyrański, M.; Krygowski, T. M.; *Tetrahedron* **1996**, *52*, 13795. [Crossref]
57. Bandyopadhyay, I.; Manogaran, S.; *J. Mol. Struct.: THEOCHEM* **2000**, *507*, 217. [Crossref]
58. Herbststein, F. H.; Schmidt, G. M. J.; *Nature* **1952**, *169*, 323. [Crossref]
59. Zendaoui, S. M.; Zouchoune, B.; *Polyhedron* **2013**, *51*, 123. [Crossref]
60. Hirshfeld, F. L.; Schmidt, G. M. J.; *J. Chem. Phys.* **1957**, *26*, 923. [Crossref]
61. Adad, A.; Hmammouchi, R.; Lakhliki, T.; Bouachrine, M.; *J. Chem. Pharm. Res.* **2013**, *5*, 26. [Link] accessed in January 5, 2023
62. Kotwica, K.; Wielgus, I.; Proń, A.; *Materials* **2021**, *14*, 5155. [Crossref]
63. Costa, J. C. S.; Taveira, R. J. S.; Lima, C. F. R. A. C.; Mendes, A.; Santos, L. M. N. B. F.; *Opt. Mater. (Amsterdam, Neth.)* **2016**, *58*, 51. [Crossref]
64. Elangovan, A.; Chiu, H. H.; Yang, S. W.; Ho, T. I.; *Org. Biomol. Chem.* **2004**, *2*, 3113. [Crossref]
65. Zhou, C.; Zhang, T.; Zhang, S.; Liu, H.; Gao, Y.; Su, Q.; Wu, Q.; Li, W.; Chen, J.; Yang, B.; *Dyes Pigm.* **2017**, *146*, 558. [Crossref]
66. Plasseraud, L.; Catey, H.; Richard, P.; Ballivet-Tkatchenko, D.; *J. Organomet. Chem.* **2009**, *694*, 2386. [Crossref]
67. Dolgounitcheva, O.; Zakrzewski, V. G.; Ortiz, J. V.; *J. Phys. Chem. A* **1997**, *101*, 8554. [Crossref]
68. Adhikari, S.; Santra, B.; Ruan, S.; Bhattarai, P.; Nepal, N. K.; Jackson, K. A.; Ruzsinszky, A.; *J. Chem. Phys.* **2020**, *153*, 184303. [Crossref]
69. Jeffrey, G. A.; Ruble, J. R.; McMullan, R. K.; Pople, J. A.; *Proc. R. Soc. A* **1987**, *414*, 47. [Crossref]
70. Brock, C. P.; Dunitz, J. D.; *Acta Crystallogr., Sect. B: Struct. Sci., Cryst. Eng. Mater.* **1982**, *B38*, 2218. [Crossref]
71. Kalescky, R.; Kraka, E.; Cremer, D.; *J. Phys. Chem. A* **2014**, *118*, 223. [Crossref]
72. Herzberg, G.; *Molecular Spectra and Molecular Structure. Vol. III: Electronic Spectra and Electronic Structure of Polyatomic Molecules*, 2nd ed.; Von Nostrand Reinhold Co.: New York, 1966.